ACS SENSORS

Article

Cite This: ACS Sens. 2019, 4, 931−937

pubs.acs.org/acssensors

Top-Down Strategy of Implantable Biosensor Using Adaptable, Porous Hollow Fibrous Membrane

Jin Zhou,[‡,∥] Zhen Ma,[§] Xiao Hong,[†] Hui-Min Wu,[†] Shu-Yan Ma,[†] Yang Li,[†] Da-Jing Chen,[*,§] Hai-Yin Yu,[*,‡] and Xiao-Jun Huang[*,†]

[†]MOE Key Laboratory of Macromolecular Synthesis and Functionalization, Department of Polymer Science and Engineering, Zhejiang University, Hangzhou 310027, China

[‡]College of Chemistry and Materials Science, Anhui Normal University, Wuhu 241000, China

[§]School of Medicine, Hangzhou Normal University, Hangzhou 311121, China

[∥]Department of Material and Chemical Engineering, Chizhou University, Chizhou 247000, China

Supporting Information

ABSTRACT: Fabrication of an outer membrane is crucial for an implantable biosensor to enhance the long-term stability and accuracy of sensors. Herein, an adaptable, controllable, porous outer membrane for an implantable biosensor was fabricated using a "top-down" method, allowing maximum retention of enzyme activity and fine control over membrane microstructure. Polysulfone hollow fibrous membranes with different pore sizes and porosities were used as a base membrane. Chitosan (CH) and sodium alginate (SA) were self-assembled on the inner surface of PSfHM to construct a biocompatible and conductive interface between PSfHM and the electrode. In vitro and in vivo experiments were used to evaluate the performance of implantable glucose biosensors with PSfHM and CH/SA modified PSfHM (PSfHM-CH/SA). The glucose biosensor with PSfHM-CH/SA exhibited a more stable output current than bare sensors and a quick response time (<50 s). The glucose biosensor with PSfHM-CH/SA linear sensing range was between 0 and 22 mM (R^2 = 0.9905), and relative sensitivity remained at >87% within 7 days and >76% within 15 days. Furthermore, response currents recorded by implanted sensors closely followed the blood glucose trend from the tail vein blood during in vivo experiments.

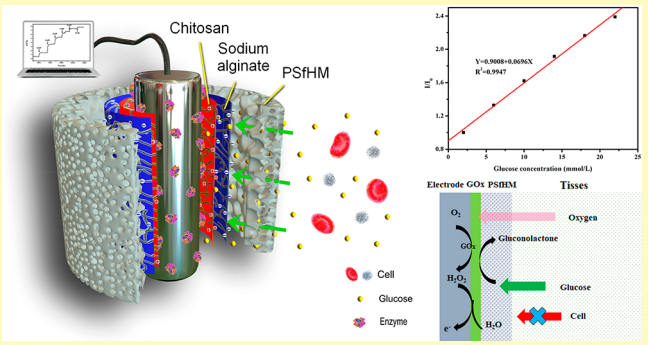

KEYWORDS: *implantable biosensor, top-down strategy, hollow fibrous membrane, polyelectrolyte, continuous glucose monitoring*

With the rapid development of device intellectualization and informatization, a wide variety of implantable intelligent devices and continuous monitoring sensors are being put into clinical application.[1−4] These play a vital role in daily life for self-monitoring and self-nursing, allowing continuous monitoring of deviations from a healthy state. Intelligent continuous monitoring sensors (ICMSs) have great potential for monitoring, diagnosing, and suggesting personalized treatment for a variety of diseases.[5] However, during clinical subcutaneous applications, implantable ICMSs face primary challenges with long-term stability[6] and accuracy.[7] Because working electrodes contact biological tissue, they might lead to direct problems for patients; for example, bioactive substances coated on the electrode surface may diffuse into the tissue fluid. The patient's immune system may also attack the implanted electrodes, damaging the coating layer (e.g., enzyme and other bioactive substances), which can result in reduced sensor lifetime in vivo.[6] In addition, interferents in tissue fluid can affect analyte measurement.[8]

In recent years, researchers have made great advances in solving the problems associated with implantable ICMSs. These include great efforts to develop noninvasive strategies including optical and electrochemical sensor to measure glucose in skin interstitial fluid and sweat. However, noninvasive wearable sensors lack reliable and stable long-term working performance compared with implantable sensors.[9,10] Compared with a noninvasive glucose sensor, implantable sensors exhibited better accuracy and stability. For minimally invasive sensors, construction of a composite multilayer by layer-by-layer coating (a "bottom-up" method) on the surface of working electrodes has been established as an effective method[11] to solve the problems in implantation. Various materials have now been introduced to fabricate the composite multilayer of membranes. Metal nanoparticles and nanopolyaniline layers can enhance the efficiency of signal outputs

Received: January 6, 2019
Accepted: April 5, 2019
Published: April 5, 2019

DOI: 10.1021/acssensors.9b00035
ACS Sens. 2019, 4, 931−937

and enzyme immobilization.[12,13] Porous and nonporous polymer film layers can limit the diffusion of interferents and protect sensors.[14] Natural polymer materials such as cellulose[15,16] and chitosan[17,18] and synthetic polymer materials such as polyurethane,[13,14,19−21] polyvinylidene fluoride,[12] polypropylene,[22] and poly(lactic acid) (PLA)[6,23] have been applied to form the outer membrane. The ideal outer membrane should have both good histocompatibility and a micronano pore size with high porosity.[11] A membrane with good histocompatibility can reduce the chance of tissue rejection,[24,25] which could otherwise lead to damage of the outer membrane, enzymes, or other constituents on the electrode surface. Micronano pore size can be used to control analyte diffusion rates and can prevent interference from unwanted molecules,[26] while high porosity can minimize mass transfer resistance and accelerate the restoration of a diffusive equilibrium state.

In contrast with well-reported "bottom-up" methods, we demonstrate a "top-down" strategy to construct an implantable biosensor. There are many advantages to using a "top-down" method: (1) precision and liberal control of membrane microstructure; (2) minimizing the influence of in situ coating on the active layer, thereby retaining optimal enzymatic activity; (3) inner and outer surface properties can be conveniently modified using filtration methods; and (4) the modified layer can absorb water when in contact with interstitial fluid, which provides a biocompatible microenvironment for bioactive substances,[27] and acts as a bridge for electron and substrate transmission from the membrane to the working electrode.

Author: Herein, hollow fibrous membranes with pore size and porosity that can be precisely regulated were kindly afforded by O'Happure Membrane Technology Co., Ltd. (Nanjing, China). The hollow fibrous membranes were further modified with hydrophilic polymer and then worn on needlelike working electrodes. In this work, a polysulfone hollow fibrous membrane (PSfHM) was applied as the outer membrane of a mini-invasive implantable biosensor. Furthermore, two polyelectrolytes, chitosan (CH) and sodium alginate (SA), were assembled on the inner surface of the PSfHM by cross-flow filtration. Implantable enzymatic amperometric glucose sensors, as the main research object in this paper, were constructed by fixing the PSfHM or CH/SA modified PSfHM (PSfHM-CH/SA) on the stainless-steel needle electrode. Linearity and sensitivity of sensors were tested by in vitro experiments in phosphate buffer solution (PBS). In vivo experiments were also performed to monitor real-time blood glucose levels following glucose and insulin injections.

MATERIALS AND METHODS

Materials and Reagents. Polysulfone hollow fibrous membranes (PSfHM) with perfect radial gradient pores (with a diameter of 0.28 mm) were afforded by O' Happure Membrane Technology Co., Ltd. (Nanjing, China). Sodium phosphate dibasic dodecahydrate, monopotassium phosphate, acetic acid, and sodium acetate were purchased from Sinopharm Chemical Reagent Co., Ltd. (Shanghai, China). Glucose oxidase was supplied by Sangon Biotech Co., Ltd. (Shanghai, China). Chitosan (viscosity: <200 mPa·S), bovine serum albumin and sodium alginate (99%) were purchased from Aladdin Industrial Corporation (Shanghai, China). Deionized water was prepared in the laboratory.

Membrane Characterization. Surface and cross-section morphologies of the PSfHM and PSfHM-CH/SA modified membrane were observed at 5 keV using field emission scanning electron microscopy (FESEM) (Hitachi S-4800, Japan). A liquid−liquid displacement porosimetry (LLDP) was employed to measure the mean pore diameter and pore diameter distribution of PSfHM. Attenuated total reflection Fourier transform infrared spectroscopy (ATR-FTIR, Nicolet, ThemoFisher, America) was carried out to determine the chemical structures of PSfHM, PSfHM-CH and PSfHM-CH/SA. X-ray photoelectron spectroscopy (XPS, PHI 5000c, PerkinElmer Instruments, U.S.A.) was implemented to compare the changes in the elemental composition of the membrane surface before and after modification. Zeta potential measurements (SurPASS 3, Anton Paar, Austria) were conducted to investigate the surface potential of the PSf membrane after assembly of Chitosan and Sodium Alginate.

Modification of the Polysulfone Hollow Fibrous Membrane by Layer-by-Layer Self-Assembly of Chitosan and Sodium Alginate. To create a stable environment for glucose oxidases, CH and SA were self-assembled layer-by-layer on the inner surface of PSfHM by a cross-flow filtration method.[28] Chitosan was dissolved in an acetic acid-sodium acetate (HAc-NaAc) buffer solution (0.2 M, pH = 5.4) to obtain a 1 mg/mL CH solution. Sodium alginate (SA) was dissolved in deionized water to obtain a 1 mg/mL solution. Eight to ten PSfHM filaments were used to form a filtration component. Self-assembly of CH and SA was proceeded by the following steps: (1) the CH solution was injected in the inner channels of the PSfHM component for 5 min by a peristaltic pump, (2) 5 mL HAc-NaAc solution (pH = 5.4) was injected in the PSfHM component to remove the loosely adsorbed CH, (3) the PSfHM components were dried by nitrogen purging for 1 min, (4) CH solution was replaced with SA solution, and then steps (1) to (3) were repeated. The final PSfHM components modified with five CH/SA bilayers were dried in a vacuum chamber overnight.

Fabrication of Glucose Biosensor Working Electrodes. Transcutaneous needle electrodes with sensor nanoparticle layers and glucose oxidase (GOx) were fabricated using a previous method from our research group.[12] Stainless steel needles with a diameter of 0.18 mm worked as a mechanical supporting substrate. The sensor nanoparticle layers were fabricated by electrodeposition. Enzyme immobilization was achieved by a liquid membrane coating method using 10% wt. glucose oxidase solution in water. The experimental details are presented in our previous research.[12]

The original and CH/SA modified PSfHM were presented on the transcutaneous needle electrodes as a sheath. Five mm PSfHM was reserved on the end of the electrode and sealed by epoxy glue. The schematic diagram and picture of the glucose biosensor are shown in Scheme 1.

Scheme 1. Schematic Diagram (left) and Picture of Implantable Glucose Biosensor (right)

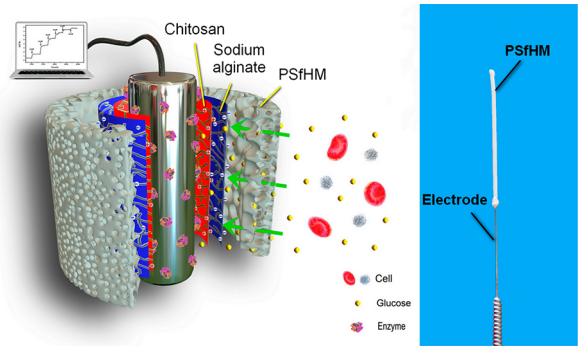

In Vitro Glucose Biosensor Experiments. Glucose biosensors with and without a PSfHM protective membrane were tested with glucose solution in phosphate buffer solution (PBS) at ambient temperature and 37 °C to evaluate the amperometric response to various glucose concentrations at 0.33 V. All electrochemical detections were made on a CHI660 electrochemical workstation at ambient temperature. PBS solution (0.2 M, pH = 7.0) was chosen as

DOI: 10.1021/acssensors.9b00035
ACS Sens. 2019, 4, 931−937

the supporting electrolyte for in vitro tests. An Ag/AgCl electrode was used as a reference electrode during in vitro tests. Glucose solution was injected into stirring PBS after current stabilization. The glucose concentration in PBS was increased by 1 mM in 1 to 10 steps and 2 mM in other steps.

The stability of sensors with original and CH/SA modified PSfHM were also characterized in in vitro tests. Sensors were stored in bovine serum at 37 °C and replaced with fresh bovine serum every day. The amperometric response at 8 mM glucose solution was measured every day during the first week and every other day during the second week.

In Vivo Glucose Biosensor Experiments. Male Sprague–Dawley mice (200 g) were narcotized with 1% pentobarbital sodium solution. PSfHM fixed sensor electrodes and Ag/AgCl reference electrode were implanted in the mouse back as shown in Figure 7a. The current response to glucose from the implanted sensors was first measured in 37 °C PBS for calibration (Figure S4). The working electrode covered with PSfHM-CH/SA was immersed in PBS for longer than 1 h before implantation to accelerate the stabilization process after implantation. The sensors were carefully slid under the skin and mechanically secured with conductive adhesive tape. The current response to glucose from the implanted sensors was measured and collected without further calibration. Glucose concentration in tail vein blood was detected synchronously using glucose testing strips. The result was compared with sensor output following each significant change in blood glucose level after glucose or insulin injection throughout the experiment. The accuracy of the glucose sensor was further evaluated by in vivo test using Clarke error grid analysis. The percent difference between the glucose sensor and actual blood glucose was calculated by standard mean absolute relative difference (MARD) protocol.

The experimental protocol was approved by the Animal Care and Use Committee of the School of Medicine, Hangzhou Normal University.

RESULTS AND DISCUSSION

Characterization of PSfHM and PSfHM-CH/SA. Membrane microstructure is crucial for sensor performance. To observe the surface and section morphology of PSfHM, PSfHM-CH/SA, field emission scanning electron microscopy (FE-SEM) was employed. Figure 1 shows the surface and cross-sectional SEM picture of blank PSfHM with different pore size and porosity. It is evident that the pore size gradually

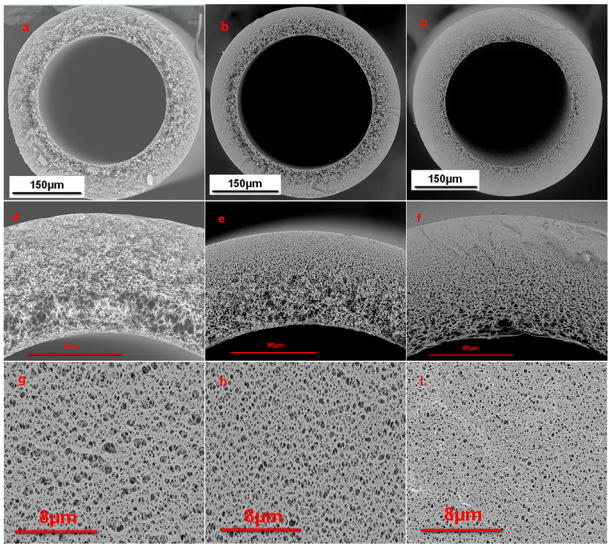

Figure 1. Surface and cross-sectional profile SEM morphology of PSfHM with mean pore size as 0.3413 μm (a,d,g), 0.5458 μm (b,e,h), and 0.7642 μm (c,f,i).

decreases from the inner surface to the outer surface. The special porous structure of PSfHM, which gradually decreases from inner surface to outer surface, can decrease the filtration resistance[29,30] while increasing the transfer efficiency of glucose. The spongelike pore structure and smaller pore diameter in outer surface can effectively intercept interferents in interstitial fluid.

The mean pore size and pore size distribution of PSfHM were measured by a liquid–liquid displacement porosimetry (LLDP) (Figure S1). Three types of PSfHM with different mean pore size (0.3413, 0.5458, and 0.7642 μm) were used as protective membranes for the glucose biosensor.

The surface and section morphology of original and CH/SA modified PSfHM are shown in Figure 2. It is clear that CH/SA

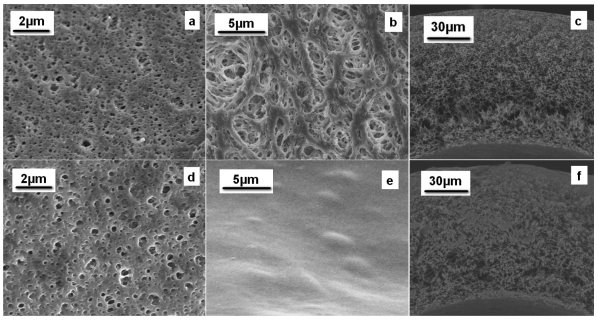

Figure 2. SEM images of outer surface, inner surface, and cross-section of PSfHM (a,b,c) and CH/SA-modified PSfHM (d,e,f).

layer were assembled on the inner surface. Research has verified that the thickness of polyelectrolyte multilayers increased with the increase in number of layer numbers.[31,32] The thickness of 10 polyelectrolyte layers is approximately 20 nm in 0.2 M pH = 5.4 PBS solution.[31] The SEM picture of CH/SA modified PSfHM indicates that the CH/SA layer is a nonporous thin film, which has been previously verified by others.[33]

The chemical groups and bases were changed after CH/SA assembling. ATR-FTIR was employed to verify the group change between PSfHM, PSfHM-CH, and PSfHM-CH/SA. The results are displayed in Figure S2. The broad peak from 3500 to 3000 cm^{-1} is attributed to characteristic peaks of hydroxyl and amino groups on chitosan and sodium alginate (Figure S2a), which is similar to findings from other research.[33] The peak intensity at 1650 and 1400 cm^{-1} of PSfHM-CH/SA was increased and attributed to the asymmetric and symmetric stretch vibrations of COO^- group in SA. This indicates the CH with amino groups and the SA with carboxylates were successfully introduced to PSfHM.

To further verify the assembly of CH/SA on the membrane, the surface elemental compositions of PSfHM, PSfHM-CH, and PSfHM-CH/SA were measured by X-ray photoelectron spectroscopy (XPS) (Table 1 and Figure 3). The nitrogen content of PSfHM-CH was 3.64% compared to 3.5% of

Table 1. Surface Elemental Composition of PSfHM, PSfHM-C, and PSfHM-C/SA

element	C	O	S	N	Na
PSfHM	75.19%	17.91%	3.4%	3.5%	0%
PSfHM-C	72.91%	19.42%	2.55%	3.64%	1.48%
PSfHM-C/SA	63.13%	31.83%	0.48%	2.67%	1.89%

DOI: 10.1021/acssensors.9b00035
ACS Sens. 2019, 4, 931–937

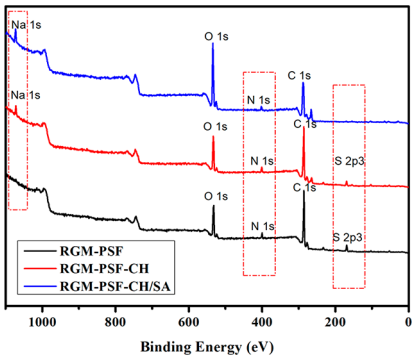

Figure 3. Surface elementary composition of blank membrane (black), modified membrane with one-layer chitosan (red), and modified membrane with one-layer chitosan and one-layer sodium alginate (blue).

PSfHM, indicating the successful adsorption of chitosan on the PSfHM surface. Sodium in PSfHM-CH and PSfHM-CH/SA spectra originated from NaAC-HAc buffer solution during the washing step and SA, respectively. The increase in oxygen content and decrease in carbon and sulfur content also verify the successful assembly of chitosan and sodium alginate on the surface of PSfHM.

The self-assembled polyelectrolyte on the surface has great influence on the zeta potential of the membrane surface. A solid surface zeta potential analyzer was applied to test the zeta potential of PSfHM before and after modification. Figure S3 presents the zeta potential of PSfHM surfaces as a function of pH value. A clear difference can be seen in zeta potential between PSfHM and PSfHM-CH. Zeta potential of PSfHM-CH was positive when the pH value was below 6, indicating the immobilization of chitosan. An evident decrease in the surface potential was observed for PSfHM-CH/SA throughout the measured pH range, which can be attributed to the presence of carboxylic ions on PSfHM-CH/SA.

Glucose Biosensor Evaluation. Sensitivity and stability, which are the two main properties of glucose sensors, can be evaluated by in vitro experiments. Three types of PSfHM with different pore sizes were used as the protective membrane of a glucose biosensor to investigate the influence of membrane pore size on sensor performance. Current−time curves (i−t curve) of glucose sensors with and without PSfHM are shown in Figure 4(1). It is clear that the i−t curve for glucose sensor with PSfHMs is smoother than that for the bare sensor, which means that sensors with PSfHM as the outer membrane produce a more stable, better linear relationships, lower current semaphore, and slightly longer response time (but still within 50 s) than the bare sensor. Figure 4(2) presents the relative current (I/I_0) versus glucose concentration in PBS of sensors with different PSfHM, ranging from 0 to 22 mM, which covers the blood glucose concentration range of diabetic patients. The calibration curves imply that PSfHM protected devices display greater linearity and current sensitivity than nonprotected sensors. The possible reason for this result is that PSfHMs can resist interferents and limit glucose diffusion. Furthermore, Figure 4(2)b to 4(2)d qualitatively indicate that the performance of glucose sensor is better (or even best) within a certain range of pore size. Because membranes with too small pore size impede the transmission of glucose from solution to the electrode surface. Conversely, membranes with large pores cannot effectively control the glucose diffusion

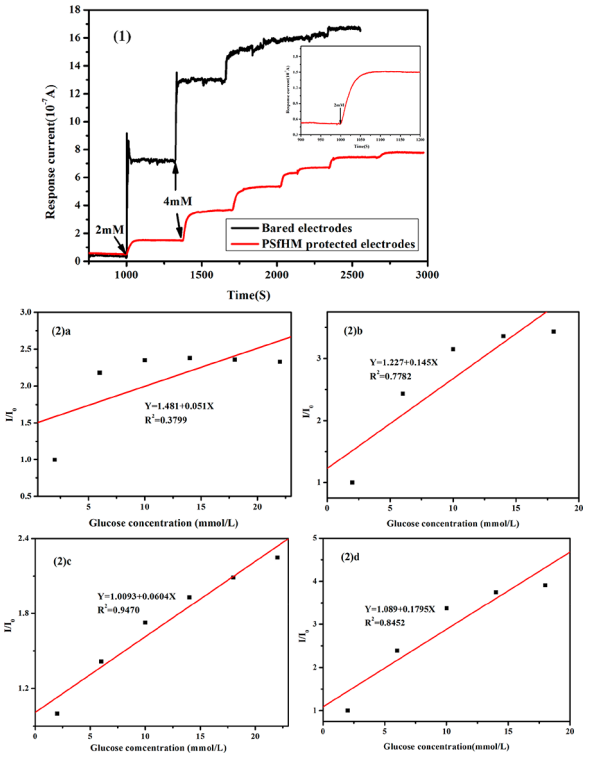

Figure 4. (1) Amperometric i−t curve of sensor without and with PSfHM; (2) sensitivity of bare glucose sensor (a), glucose sensors with PSfHM of pore size 0.7642 μm (b), 0.5458 μm (c), and 0.3413 μm (d).

through the membrane. A sensor with a suitable pore size of PSfHM can reach an equilibrium state of diffusion and restriction of glucose, presents an optimal sensor performance.

CH and SA were assembled on the inner surface of PSfHM by a cross-flow filtration method in order to regulate the membrane microstructure. This allowed us to modify inner and outer surface properties, retain optimal enzymatic activity, provide a biocompatible microenvironment for bioactive substance, and enhance the electron and mass transmission between PSfHM and sensor electrode. After the sensor protective membrane was modified with CH/SA, the current semaphore reduced, and the linearity became more pronounced, ranging from 0 to 22 mM (R^2 = 0.9905) (Figure 5). These results indicate that the CH/SA layers can further improve the performance of glucose sensors. The possible reasons are as follows: first, the microstructures and properties of PSfHM have been further modified with CH/SA layers. Second, enzyme activity can be maintained at the highest level because there is no direct contact between the enzyme and the

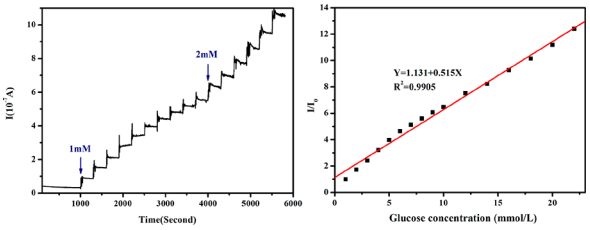

Figure 5. Amperometric i−t curve (left) and sensitivity (right) of sensors protected by PSfHM-CH/SA in PBS solution at environment temperature.

DOI: 10.1021/acssensors.9b00035
ACS Sens. 2019, 4, 931−937

solvent during the top-down fabrication process. Third, the swelling of the CH/SA multilayer can more effectively limit the transmission of glucose and increase the transmission efficiency of electrons from PSfHM to the working electrode. Finally, the swollen CH/SA multilayer can provide a biocompatible microenvironment for glucose oxidase and reduce the loss of enzyme molecules.[34]

The long-term stability of a glucose biosensor is crucial for continuous glucose monitoring. Stability detection of sensors with PSfHM and PSfHM-CH/SA were also performed during in vitro experiments (Figure 6). The retention activity of the

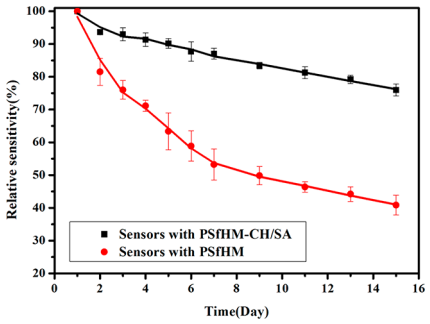

Figure 6. Response current attenuation of sensors in bovine serum at 37 °C. (The black circular dots represent the sensor with blank PSfHM, and the red square dots represent the sensor with PSfHM-CH/SA.)

bare sensor in 8 mM glucose solution declined rapidly from the first to the seventh day and then plateaued at approximately 40%. For PSfHM-CH/SA protected sensors, retention activity is decreased slowly within 7 days and then tended to remain stable from days 8 to 15. The retention sensitivity of glucose sensors with PSfHM and 5 bilayer CH/SA modified PSfHM are approximately 40% and 76% of the initial sensitivity, respectively. It is evident that sensors with PSfHM-CH/SA have higher stability than sensors with PSfHM (Figure 6), which can be attributed to two possible reasons: (1) the CH/SA layer prevented the protein from diffusing from solution to the surface of electrode, which may adsorb on the surface of glucose oxidase, causing the reduction of enzymatic activity.[24] (2) the hydrophilic CH/SA layers can form a swollen polyelectrolyte state, which can provide a biocompatible microenvironment for glucose oxidase, and improve the transmission efficiency of glucose.[35]

A glucose sensor with PSfHM-CH/SA was tested in vivo to evaluate its monitoring capability for changes in blood glucose concentration. The response current from glucose concentration was detected by implanting the sensor in mice (Figure 7). Sensor responses to intraperitoneal glucose solution injection (1.2 mg/g) are shown in Figure 7b. Response current closely follows the discrete blood glucose trend. It rose gradually after glucose injection and then became stable after 35 min. Sensor responses to insulin injection (1 U/kg) can be seen in Figure 7c. Sensor current decreases rapidly after injection and maintains its low level. A similar drop is observed in tail blood test. Figure 7b,c shows the current response and discrete blood glucose trend following the injection of glucose and insulin, respectively. With reference to the original current signal, both comparisons demonstrate that the implanted sensor can effectively monitor blood glucose changes. The accuracy of glucose sensor was further evaluated by in vivo test using Clarke error grid analysis[36] as shown in Figure 7d. It is evident that most points were in zone A. Zone A represents glucose values that deviate from the reference method by no more than 20%. Values falling within this range are clinically accurate in that they would lead to clinically correct treatment decisions.[37] Mean absolute relative difference values for validation were also <20% as listed in Table 2. Experiments for monitoring a wider range of blood glucose levels will be carried out using a diabetic mouse model further.

Table 2. Mean Absolute Relative Difference Values for Validation of In Vivo Transcutaneous Glucose Detection

rat number	points used for validation	MARDV (%)
1	8	19.07
2	8	11.92
3	6	12.50

CONCLUSIONS

In this paper, a top-down strategy was used to fabricate an implantable biosensor using an adaptable, controllable, porous hollow fibrous membrane as the outer membrane. PSfHMs with varying pore size and porosity were created and modified on their inner surface with self-assembling chitosan and sodium alginate. This was then fixed onto a working electrode. Enzymes and other biomolecules can be protected from organic solvent using dip-coating and/or modification process. The multilayered CH/SA can form a transmission bridge for matter and electrons between the membrane and electrodes to enhance the sensitivity and stability of a glucose sensor. After modification with CH/SA, the linear sensing range was from 0 to 22 mM (R^2 = 0.9905), and the relative sensitivity was greater than 87% within 7 days and 76% within 15 days.

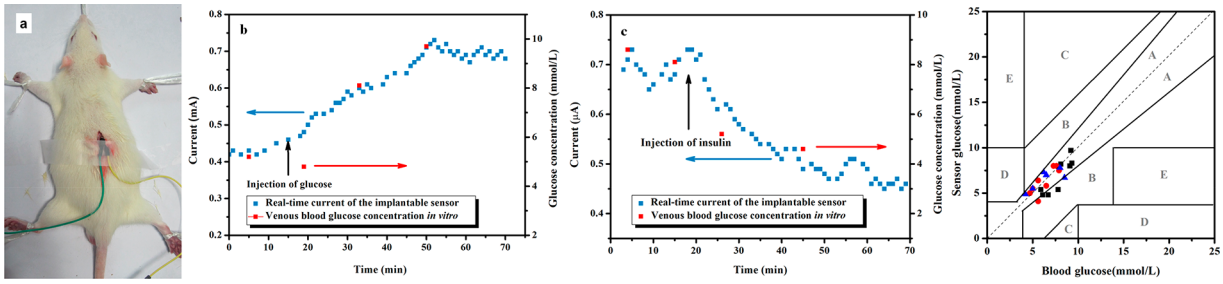

Figure 7. In vivo continuous monitoring of glucose in mice. (a) Image of transcutaneous glucose sensor attachment to mice back. (b) Implanted sensor current response to glucose injection and tail vein blood test. (c) Implanted sensors response to insulin injection and tail vein blood test. (d) In vivo transcutaneous glucose validation data sets on three rats.

DOI: 10.1021/acssensors.9b00035
ACS Sens. 2019, 4, 931−937

Response current of the sensor in vivo closely followed the blood glucose trend from mouse tail vein blood. Our results demonstrate that a reliable and high-powered sensor can be constructed by top-down fabrication of a hollow fibrous membrane on the electrode surface.

Polyelectrolyte multilayer films assembled on the inner surface of hollow fibrous membranes are crucial for improving implantable biosensor performance. It is convenient and efficient to fabricate implantable continuous monitoring of biosensors using a top-down strategy. Advantages include precision and liberal control of membrane microstructure, convenient modification of inner and outer surface properties in advance by filtration, and full retention of enzyme activity and active layers. In conclusion, hollow fibrous membranes modified with polyelectrolyte multilayers have significant potential in implantable biosensor and other medical device applications.

■ ASSOCIATED CONTENT

Supporting Information

The Supporting Information is available free of charge on the ACS Publications website at DOI: 10.1021/acssensors.9b00035.

Pore size distribution (Figure S1), attenuated total reflection infrared spectrogram (ATR-IR) (Figure S2), Zeta potential dependence on pH (Figure S3) of different membranes, and calibration of sensor in PBS solution at 37 °C (Figure S4) (PDF)

■ AUTHOR INFORMATION

Corresponding Authors

*E-mail: hxjzxh@zju.edu.cn. Tel:0571-88276294. Fax:0571-85719641.
*E-mail: yhy456@mail.ahnu.edu.cn
*E-mail: djchen@hznu.edu.cn

ORCID

Hai-Yin Yu: 0000-0002-6478-4137
Xiao-Jun Huang: 0000-0003-4682-7364

Author Contributions

X.H., S.-Y.M.: Measurement of the pore size and porosity of membranes. H.-M.W.: Infrared spectroscopic analysis of membranes. J.Z.: Modification and characterization of PSfHM, fabrication of glucose sensor, in vitro performance test of glucose sensor, and paper writing. Z.M.: In vivo performance test of glucose sensor. Y.L.: Modification of the article. D.-J.C.: In vivo performance test of glucose sensor, modification of the article, and corresponding author. X.-J.H.: Proposing research proposals and writing outline, corresponding author. H.-Y.Y.: XPS analysis of membranes, corresponding author.

Notes

The authors declare no competing financial interest.

■ ACKNOWLEDGMENTS

This research was supported by the Fundamental Research Funds for the Central Universities of China (Contract Grant No. 2018QNA4057), Natural Science Foundation of China (Grant Nos. 61801160, 21371008, and 51473143), and Zhejiang Provincial Natural Science Foundation of China (Grant No. LY18H180009).

■ REFERENCES

(1) Darwish, A.; Hassanien, A. E. Wearable and implantable wireless sensor network solutions for healthcare monitoring. *Sensors* **2011**, *11*, 5561−5595.
(2) Ma, Y.; Zheng, Q.; Liu, Y.; Shi, B.; Xue, X.; Ji, W.; Liu, Z.; Jin, Y.; Zou, Y.; An, Z.; Zhang, W.; Wang, X.; Jiang, W.; Xu, Z.; Wang, Z. L.; Li, Z.; Zhang, H. Self-Powered, One-Stop, and Multifunctional Implantable Triboelectric Active Sensor for Real-Time Biomedical Monitoring. *Nano Lett.* **2016**, *16*, 6042−6051.
(3) Mariacher, S.; Ebner, M.; Januschowski, K.; Hurst, J.; Schnichels, S.; Szurman, P. Investigation of a novel implantable suprachoroidal pressure transducer for telemetric intraocular pressure monitoring. *Exp. Eye Res.* **2016**, *151*, 54−60.
(4) Sharma, T.; Naik, S.; Langevine, J.; Gill, B.; Zhang, J. X. J. Aligned PVDF-TrFE Nanofibers With High-Density PVDF Nanofibers and PVDF Core-Shell Structures for Endovascular Pressure Sensing. *IEEE Trans. Biomed. Eng.* **2015**, *62*, 188−195.
(5) Gifford, R. Continuous glucose monitoring: 40 years, what we've learned and what's next. *ChemPhysChem* **2013**, *14*, 2032−2044.
(6) Fang, L.; Liang, B.; Yang, G.; Hu, Y.; Zhu, Q.; Ye, X. Study of glucose biosensor lifetime improvement in 37°C serum based on PANI enzyme immobilization and PLGA biodegradable membrane. *Biosens. Bioelectron.* **2014**, *56*, 91−96.
(7) Kropff, J.; Choudhary, P.; Neupane, S.; Barnard, K.; Bain, S. C.; Kapitza, C.; Forst, T.; Link, M.; Dehennis, A.; DeVries, J. H. Andrew Dehennis, Accuracy and Longevity of an Implantable Continuous Glucose Sensor in the PRECISE Study_ A 180-Day, Prospective, Multicenter, Pivotal Trial. *Diabetes Care* **2017**, *40*, 63−68.
(8) Lorenz, C.; Sandoval, W.; Mortellaro, M. Interference Assessment of Various Endogenous and Exogenous Substances on the Performance of the Eversense Long-Term Implantable Continuous Glucose Monitoring System. *Diabetes Technol. Ther.* **2018**, *20*, 344−352.
(9) Rachim, V. P.; Chung, W.-Y. Wearable-band type visible-near infrared optical biosensor for non-invasive blood glucose monitoring. *Sens. Actuators, B* **2019**, *286*, 173−180.
(10) Kim, J.; Campbell, A. S.; Wang, J. Wearable non-invasive epidermal glucose sensors: A review. *Talanta* **2018**, *177*, 163−170.
(11) Wang, N.; Burugapalli, K.; Song, W.; Halls, J.; Moussy, F.; Ray, A.; Zheng, Y. Electrospun fibro-porous polyurethane coatings for implantable glucose biosensors. *Biomaterials* **2013**, *34*, 888−901.
(12) Chen, D.; Wang, C.; Chen, W.; Chen, Y.; Zhang, J. X. J. PVDF-Nafion nanomembranes coated microneedles for in vivo transcutaneous implantable glucose sensing. *Biosens. Bioelectron.* **2015**, *74*, 1047−1052.
(13) Fang, L.; Liang, B.; Yang, G.; Hu, Y.; Zhu, Q.; Ye, X. A needle-type glucose biosensor based on PANI nanofibers and PU/E-PU membrane for long-term invasive continuous monitoring. *Biosens. Bioelectron.* **2017**, *97*, 196−202.
(14) Yu, B.; Long, N.; Moussy, Y.; Moussy, F. A long-term flexible minimally-invasive implantable glucose biosensor based on an epoxy-enhanced polyurethane membrane. *Biosens. Bioelectron.* **2006**, *21*, 2275−2282.
(15) Esmaeili, C.; Abdi, M.; Mathew, A.; Jonoobi, M.; Oksman, K.; Rezayi, M. Synergy Effect of Nanocrystalline Cellulose for the Biosensing Detection of Glucose. *Sensors* **2015**, *15*, 24681−24697.
(16) Ren, X.; Chen, D.; Meng, X.; Tang, F.; Du, A.; Zhang, L. Amperometric glucose biosensor based on a gold nanorods/cellulose acetate composite film as immobilization matrix. *Colloids Surf., B* **2009**, *72*, 188−192.
(17) Şenel, M. Simple method for preparing glucose biosensor based on in-situ polypyrrole cross-linked chitosan/glucose oxidase/gold bionanocomposite film. *Mater. Sci. Eng., C* **2015**, *48*, 287−293.
(18) Zhang, Y.; Li, Y.; Wu, W.; Jiang, Y.; Hu, B. Chitosan coated on the layers' glucose oxidase immobilized on cysteamine/Au electrode for use as glucose biosensor. *Biosens. Bioelectron.* **2014**, *60*, 271−276.
(19) Koh, A.; Lu, Y.; Schoenfisch, M. H. Fabrication of nitric oxide-releasing porous polyurethane membranes-coated needle-type implantable glucose biosensors. *Anal. Chem.* **2013**, *85*, 10488−10494.

DOI: 10.1021/acssensors.9b00035
ACS Sens. 2019, 4, 931−937

(20) Vallejo-Heligon, S. G.; Brown, N. L.; Reichert, W. M.; Klitzman, B. Porous, Dexamethasone-loaded polyurethane coatings extend performance window of implantable glucose sensors in vivo. *Acta Biomater.* **2016**, *30*, 106−115.
(21) Wang, N.; Burugapalli, K.; Wijesuriya, S.; Far, M. Y.; Song, W.; Moussy, F.; Zheng, Y.; Ma, Y.; Wu, Z.; Li, K. Electrospun polyurethane-core and gelatin-shell coaxial fibre coatings for miniature implantable biosensors. *Biofabrication* **2014**, *6*, 015002.
(22) Fortin, N.; Klok, H.-A. Glucose Monitoring Using a Polymer Brush Modified Polypropylene Hollow Fiber-based Hydraulic Flow Sensor. *ACS Appl. Mater. Interfaces* **2015**, *7*, 4631−4640.
(23) Koschwanez, H. E.; Yap, F. Y.; Klitzman, B.; Reichert, W. M. In vitro and in vivo characterization of porous poly-L-lactic acid coatings for subcutaneously implanted glucose sensors. *J. Biomed. Mater. Res., Part A* **2008**, *87A*, 792−807.
(24) Hu, Y.; Yang, G.; Liang, B.; Fang, L.; Ma, G.; Zhu, Q.; Chen, S.; Ye, X. The fabrication of superlow protein absorption zwitterionic coating by electrochemically mediated atom transfer radical polymerization and its application. *Acta Biomater.* **2015**, *13*, 142−149.
(25) Chen, C.-C.; Wu, C.-H.; Wu, J.-J.; Chiu, C.-C.; Wong, C.-H.; Tsai, M.-L.; Lin, H.-T. V. Accelerated bioethanol fermentation by using a novel yeast immobilization technique: Microtube array membrane. *Process Biochem.* **2015**, *50*, 1509−1515.
(26) Bisht, R.; Jaiswal, J. K.; Chen, Y.-S.; Jin, J.; Rupenthal, I. D. Light-responsive in situ forming injectable implants for effective drug delivery to the posterior segment of the eye. *Expert Opin. Drug Delivery* **2016**, *13*, 953−962.
(27) Niepel, M. S.; Mano, J. F.; Groth, T. Effect of Polyelectrolyte Multilayers Assembled on Ordered Nanostructures on Adhesion of Human Fibroblasts. *ACS Appl. Mater. Interfaces* **2016**, *8*, 25142−25151.
(28) Zhang, G.; Song, X.; Ji, S.; Wang, N.; Liu, Z. Self-assembly of inner skin hollow fiber polyelectrolyte multilayer membranes by a dynamic negative pressure layer-by-layer technique. *J. Membr. Sci.* **2008**, *325*, 109−116.
(29) Zhu, X.-Y.; Chen, C.; Chen, P.-C.; Gao, Q.-L.; Fang, F.; Li, J.; Huang, X.-J. High-performance enzymatic membrane bioreactor based on a radial gradient of pores in a PSF membrane via facile enzyme immobilization. *RSC Adv.* **2016**, *6*, 30804−30812.
(30) Guo, Y.; Zhu, X.; Fang, F.; Hong, X.; Wu, H.; Chen, D.; Huang, X. Immobilization of Enzymes on a Phospholipid Bionically Modified Polysulfone Gradient-Pore Membrane for the Enhanced Performance of Enzymatic Membrane Bioreactors. *Molecules* **2018**, *23*, 144.
(31) Boddohi, S.; Killingsworth, C. E.; Kipper, M. J. Polyelectrolyte multilayer assembly as a function of pH and ionic strength using the polysaccharides chitosan and heparin. *Biomacromolecules* **2008**, *9*, 2021−2028.
(32) Yuan, W.; Fu, J.; Su, K.; Ji, J. Self-assembled chitosan/heparin multilayer film as a novel template for in situ synthesis of silver nanoparticles. *Colloids Surf., B* **2010**, *76*, 549−555.
(33) Wang, H.; Zhao, X.; He, C. Constructing a novel zwitterionic surface of PVDF membrane through the assembled chitosan and sodium alginate. *Int. J. Biol. Macromol.* **2016**, *87*, 443−448.
(34) Senel, M. Simple method for preparing glucose biosensor based on in-situ polypyrrole cross-linked chitosan/glucose oxidase/gold bionanocomposite film. *Mater. Sci. Eng., C* **2015**, *48*, 287−293.
(35) Hu, Y.; Liang, B.; Fang, L.; Ma, G.; Yang, G.; Zhu, Q.; Chen, S.; Ye, X. Antifouling Zwitterionic Coating via Electrochemically Mediated Atom Transfer Radical Polymerization on Enzyme-Based Glucose Sensors for Long-Time Stability in 37 °C Serum. *Langmuir* **2016**, *32*, 11763−11770.
(36) Stockl, D.; Dewitte, K.; Fierens, C.; Thienpont, L. M. Evaluating clinical accuracy of systems for self-monitoring of blood glucose by error grid analysis - Comment on constructing the ″upper A-line″. *Diabetes Care* **2000**, *23*, 1711−1712.
(37) Clarke, W. L.; Cox, D.; Gonder-Frederick, L. A.; Carter, W.; Pohl, S. L. Evaluating clinical accuracy of systems for self-monitoring of blood glucose. *Diabetes Care* **1987**, *10*, 622−628.

DOI: 10.1021/acssensors.9b00035
ACS Sens. 2019, 4, 931−937